CHAPTER IV
THERMAL, MECHANICAL, AND ANTIMICROBIAL PROPERTIES OF SILVER-COATED WET-SPUN ALGINATE FIBERS

4.1 Abstract

Antibacterial alginate fibers were prepared by coating silver particles on the fibers via the wet spinning process. Effect of the silver on structure, thermal stability, surface morphology, and mechanical behavior of the fibers was characterized. Interestingly, the occurrence of silver nanoparticles can be achieved by using small proportion of the silver coated on the fibers. Moreover, at these compositions, the good distribution of silver nanoparticles was observed resulting in the enhancement of the mechanical properties of the fibers. These fibers showed antibacterial activities against both gram-positive *Staphylococcus aureus* and gram-negative *Escherichia coli* because of the presence of silver particles.

(Key-words: alginate; silver nitrate; wound dressing; antibacterial activity)

4.2 Introduction

Polysaccharide-based dressings have increasingly become viable alternatives to somewhat incompatible and often problematic cotton or viscose rayon gauzes traditionally used as wound dressings (Miraftab *et al.*, 2003). Among the various fibrous and hydrogel products, alginate-based products are the most popular ones used in wound management (Horncastle, 1995; Qin and Gilding, 1996). Alginate is a natural biopolymer obtained from cell walls of brown algae or phaeophytes such as *Laminaria* sp. and *Ascophyllum* sp. seaweeds (Clare, 1993). Alginate is a linear copolymer with homopolymeric blocks of (1-4)-linked β-D-mannuronate (M) and its C-5 epimer α-L-guluronate (G) residues, respectively, covalently linked together in different sequences or blocks (Anonymous, 2007). The monomers can appear in homopolymeric blocks of consecutive G-residues (G-

blocks), consecutive M-residues (M-blocks), alternating M and G-residues (MG-blocks) or randomly organized blocks.

Alginate can dissolve in water and, in the presence of Ca^{2+} cations, alginate gels can be formed due to ionic cross-linking via calcium bridges between L-guluronate residues on adjacent chains (McDowell, 1974). This renders alginate its reversible solubility in aqueous media and is proven instrumental in its development as fibers. Alginate-based products offer many advantages as they are biocompatible and readily form gels upon absorption of wound exudates. This eliminates fiber entrapment in the wound, which is a major cause of patient trauma/discomfort during dressing removal. Such gels prevents the wound surface from drying out, which is beneficial since a moist wound environment promotes healing and leads to a better cosmetic repair of the wound (Winter, 1962). Moreover, alginate has been known to exhibit a haemostatic function (Jarvis *et al.*, 1987) and is capable of absorbing specific solutes. As a result, it is considered as a suitable component for modern wound management aids (Lloyd *et al.*, 1998). However, alginate itself does not possess an antimicrobial property and wounds often provide favorable environments for colonization of microorganisms, which may lead to infection and delayed healing.

Therefore, in designing a material that promotes wound healing, the ability of the material in providing an adequate antimicrobial activity is desirable, provided that the antimicrobial agent present does not compromise its healing abilities (Guggenbichler *et al.*, 1999). Ionic silver is one of the most commonly used antimicrobial agents, exhibiting activity against a broad range of microorganisms (Galeano *et al.*, 2003; Gaonkar *et al.*, 2003; Thomas and McCubbin, 2003). As a consequence, silver salts and compounds have been widely used as environmental biocides and clinical antimicrobial agents (Clement and Jarrett, 1994; George *et al.*, 1997; Gupta, and Silver, 1998). The use of silver in wound-care products is commercially available, e.g., Hydrofiber® and Acticoat™ dressings (Percival *et al.*, 2005; Dunn and Jones, 2004). The inhibitory action of silver ions towards microbes supposedly derives from their bindery with the negatively-charged microbial proteins, preventing their replication, or from the attachment to sulfhydryl groups, preventing their respiration, thus inhibiting their proliferation (Holt and Bard, 2005; Bragg and Rainnie, 1974; Darouiche, 1999).

Based on the above considerations, the main objective of the present contribution was to develop a wound dressing material that combines the good characteristics of both alginate and silver. Such a material was fabricated in the form of fibers by a wet spinning process. Impartation of the antimicrobial activity to the wet-spun alginate fibers was done by silver coating. The effect of the silver coating on the structure, thermal stability, surface morphology, mechanical behavior, and, finally, antibacterial activity of the silver-coated alginate fibers was thoroughly investigated.

4.3 Experimental

4.3.1 Materials

Sodium alginate in the form of white powder was purchased from Carlo Erba (Italy). Silver nitrate ($AgNO_3$; analytical reagent grade) was purchased from Fisher Scientific (USA). Dehydrated calcium chloride ($CaCl_2$; edible grade) was purchased from Asia Drug & Chemical (Thailand). Methanol, ethanol, and acetone (commercial grade) were purchased from Labscan (Asia, Thailand). All other chemicals were of reagent grade and used as received.

4.3.2 Preparation of Silver-Coated Alginate Fibers by Wet-Spinning

A sodium alginate solution at a fixed concentration of 6% w/v was prepared by dissolving a weighed amount of sodium alginate powder in distilled water. The as-prepared sodium alginate solution was left standing in room condition for degassing prior to further fabrication into fibers. Wet-spinning was used to fabricate the fibers. The spinning solution was extruded under pressure (~6.86×10^4 $N \cdot m^{-2}$ by pressurized air) through a spinneret (composed of 30 holes with the diameter of each hole being 0.20 mm) into a series of coagulation baths (1 m in length), with the first coagulation bath containing 5% w/v $CaCl_2$ in 50% v/v methanol aqueous solution and the second coagulation baths containing various amounts of $AgNO_3$ (i.e., 0, 0.2, 0.4, 0.6, 0.8, and 1.0% w/v) in 80% v/v methanol aqueous solution. The use of the second coagulation bath was to impart the

antimicrobial activity to the obtained alginate fibers. After leaving the second coagulation bath, each yarn was drawn between two sets of rollers at a draw ratio of about 1.16 and was finally collected by a winder on a bobbin. The yarn was then washed several times with methanol and dried for 24 h in air at room condition. After drying, the yarns were cut perpendicular to their alignment to remove from the bobbin and later stored in a sealed plastic bag for further characterization. For most tests except for Fourier transformed infrared spectroscopy (FT-IR) and mechanical testing, the cut yarns for each type of samples kept in the plastic bags were used.

4.3.3 Characterization

4.3.3.1 Chemical Integrity

Neat and silver-coated alginate films were prepared from 6% w/v sodium alginate solution by casting a metered volume of the solution (i.e., 7 cm^3) in petri dishes, followed by immediate immersion in the first coagulation bath containing 5% w/v $CaCl_2$ in a 50% v/v methanol aqueous solution and later in the second coagulation bath containing various amounts of $AgNO_3$ (i.e., 0, 0.2, 0.4, 0.6, 0.8, and 1.0% w/v) in 80% v/v methanol aqueous solution. The films were dried for 24 h in air at room condition and kept in sealed plastic bags prior to further investigation by FT-IR. AgCl powder was prepared by mixing 0.5 g of silver nitrate and 0.5 g of calcium chloride in distilled water to get precipitated AgCl. The precipitant was then dried at 60°C for 6 h to remove water. This precipitated AgCl exibited grey color. AgCl powder was then mixed with KBr to make a pellet.

FT-IR spectra of sodium alginate powder, alginate film, silver-coated alginate films, silver nitrate powder and silver chloride powder were collected by a Thermo Nicolet Nexus 670 FT-IR spectrophotometer with 64 scans at a resolution of 4 cm^{-1} over a frequency range of 4000-400 cm^{-1} using deuterated triglycinesulfate (DTGS) detector.

4.3.3.2 Thermal and Physical Integrity

Thermal stability of the neat and the silver-coated alginate yarns were characterized by a Perkin-Elmer thermogravimatric/differential thermal analyzer (TG/DTA). About 10 mg of each yarn sample was analyzed over a temperature range of 30 to 700°C at a fixed heating rate of 10°C·min^{-1} under a

nitrogen atmosphere. Physical appearance of the neat and the silver-coated alginate yarns was observed by a JEOL JSM-5200 scanning electron microscopy (SEM), operating at 15 kV at a magnification of 500x. The average diameters of the individual fibers were determined from at least 100 fibers, using an image-analytical software (SemAfore 4.0). The content of silver aggregates on the fiber surfaces was investigated using an energy-dispersive spectroscopy (EDS) after carbon coating and the size of these silver aggregates was measured by the same image-analytical software as for the fiber diameters.

4.3.3.3 Mechanical Integrity

Each of the neat and the silver-coated alginate yarns were cut into rectangular specimens (i.e., 30 cm in length). These specimens were first dried in an oven at 40°C for 2 h and then weighed by a Mettler AE163 five-decimal balance. The linear density of the yarns was expressed in tex (i.e., the mass in g per 1000 m of a yarn). The mechanical integrity of the yarns in terms of the tenacity and the elongation at break was measured according to the instructions set forth in the ISO 2062:1993 standard test method. The load cell, the gauge length, and the displacement rate were 100 N, 50 mm, and 50 mm/min, respectively. The results were reported as average values from 30 specimens. Both the temperature and the relative humidity, during the measurements, were controlled at 25 ± 2°C and 55 ± 2%, respectively.

4.3.4 Antibacterial Test

Antibacterial property of the neat and the silver-coated alginate yarns were evaluated based on the parallel streak method according to the AATCC 147:1998 standard test method. The yarns were cut into rectangular specimens (i.e., 1.5 cm × 4 cm). These were test against gram-positive *Staphylococcus aureus* (*S. aureus*) and gram-negative *Escherichia coli* (*E. coli*). Briefly, 15 ml of sterilized nutrient agar was dispensed onto Petri dishes. Inoculum was prepared by transferring one colony of each microorganism into 20 ml of broth solution. The mixtures were cultured at 37°C in a shaking incubator for 24 h. An inoculating loop was used to transfer the diluted inoculum to the surface of the sterile agar. Three

parallel streaks of ~60 mm in length and ~10 mm apart were made, with each streak being prepared from 1 full load of inoculum on the inoculating loop. Each yarn specimen was then put on top of the inoculum streaks, with fiber axis being placed perpendicular to the streaks. The neat alginate yarn was used as control. The Petri dishes were incubated at 37°C for 24 h. Each type of yarn was evaluated three times. The widths of the clear zone along the inoculum streaks on both sides of each specimen were measured using a Starrett 727 digital caliper and these values were averaged to give an average value for the particular specimen.

4.4 Results and Discussion

4.4.1 Chemical Integrity

FT-IR spectra of sodium alginate powder, neat alginate film, and silver-coated alginate films are shown in Figure 4.1. Those of $AgNO_3$ and AgCl powder are also shown for comparison.

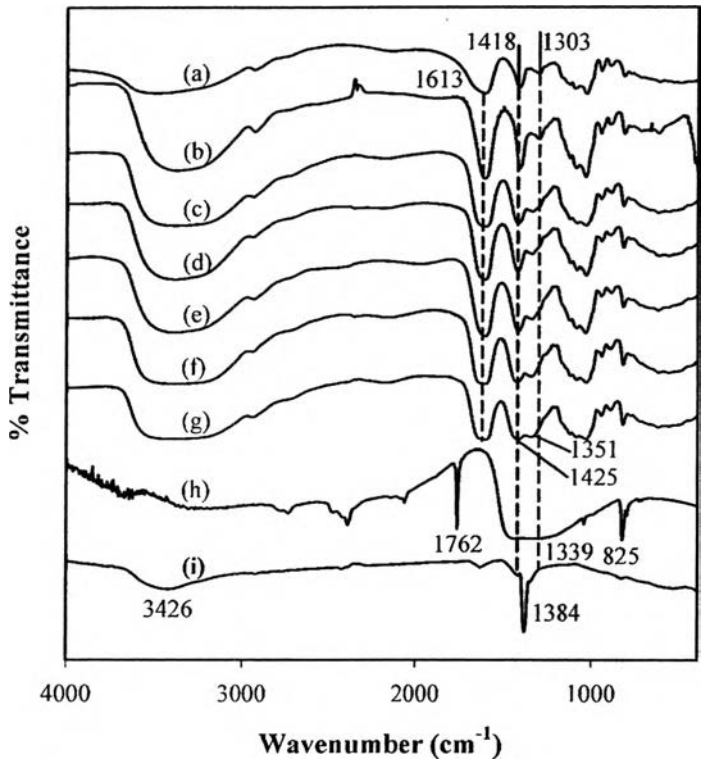

Figure 4.1 FTIR spectra of (a) alginate powder, (b) neat alginate film, silver-coated alginate films with (c) 0.2%, (d) 0.4%, (e) 0.6%, (f) 0.8%, (g) 1.0% w/v of silver nitrate, (h) silver nitrate powder and (i) silver chloride powder.

The FT-IR spectrum of sodium alginate powder shows the characteristic absorption bands at 1613 and 1418 cm^{-1}, corresponding to the asymmetric and symmetric stretching of COO^- groups, respectively (Kodokawa *et al.*, 2005). For neat alginate film, these two peaks were also observed, but the absorption band characteristic to the COO^- groups (i.e., 1613 cm^{-1}) was shifted to a lower value (i.e., 1610 cm^{-1}), due likely to the binding with Ca^{2+} (Ribeiro *et al.*, 2005). For $AgNO_3$ powder, there are two sharp absorption peaks at 1762 and 825 cm^{-1} and a broad absorption band at 1339 cm^{-1}, corresponding to NO_3^- (Lever *et al.*, 1971), while there is a broad absorption band at 3426 cm^{-1} and one sharp absorption peak at 1384 cm^{-1} for precipitated AgCl particles. For silver-coated alginate films, the peaks characteristic to both $AgNO_3$ and AgCl particles were not observed, while the peak characteristic to COO^- groups became broaden and slightly shifted (from that of the

neat alginate powder and film, i.e., 1418 cm^{-1} → 1421-1426 cm^{-1}), with the extent of the broadening and the shifting being found to increase with increasing the $AgNO_3$ concentration in the 2nd coagulation bath. The broadening of the 1608-1609 cm^{-1} band and the shifting of the 1421-1426 cm^{-1} peak may relate to further binding of the COO^- groups with Ag^+ (Kwon *et al.*, 2005).

4.4.2 Thermal Integrity

Figure 4.2 shows DSC thermograms of sodium alginate powder, neat alginate yarn, and silver-coated alginate yarns. That of $AgNO_3$ powder is also shown for comparison. The DSC thermogram of native sodium alginate powder exhibited an endotherm and an exotherm at 93 and 251°C, respectively. These observations compared well with those reported by others (Miura *et al.*, 1999; Smitha *et al.*, 2005). These two peaks, though slightly shifted (i.e., 110 and 230°C), were also visible in the DSC thermogram of neat alginate yarn, with additional peak being observed at 284°C. Such an additional peak was also reported by others (Ribeiro *et al.*, 2005). These three peaks, though slightly shifted, were also visible in the DSC thermograms of silver-coated alginate yarns, with an additional peak being observed at a high-temperature region (i.e., 317-331°C). The endotherms observed for sodium alginate powder, neat alginate yarn, and silver-coated alginate yarns should correspond to the loss of absorbed moisture (Zohuriaan and Shokrolahi, 2004). Interestingly, the exothermic peak for sodium alginate powder occurred over a much greater temperature range than that of the neat alginate yarn. The large exothermic peak was thought to relate to the thermal scission of the COO^- groups and the evolution of CO_2 from the corresponding carbohydrate backbone (Shimizu and Takada, 1997). With regards to the thermogram of $AgNO_3$ powder, the three endothermic peaks observed at 171, 208, and 511°C corresponded to the solid state transition, the melting, and the decomposition temperatures, respectively (Zamali *et al.*, 1998; Anonymous, 2007).

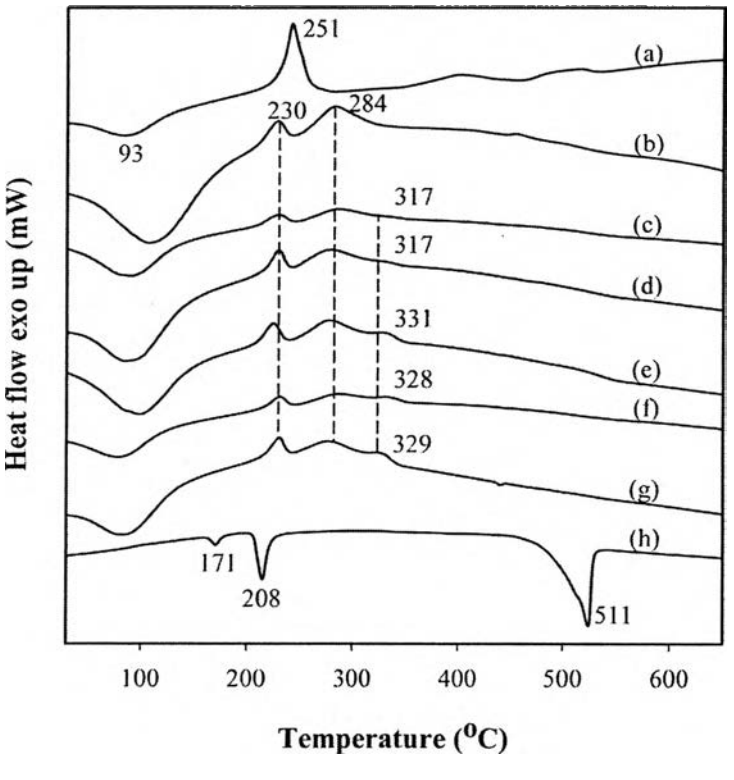

Figure 4.2 DSC thermograms of (a) alginate powder, (b) neat alginate yarn, silver-coated alginate yarns with (c) 0.2%, (d) 0.4%, (e) 0.6%, (f) 0.8%, (g) 1.0% w/v of silver nitrate, and (h) silver nitrate powder.

The thermogram of all silver-coated fibers showed the transition temperatures similar to that of the alginate fiber, in addition, the other transition temperatures occurred at around 317 °C - 331 °C. This reason may be because silver nitrate is well known to decompose at 444 °C by the following reaction:

$$2AgNO_3 \xrightarrow[\Delta]{} 2Ag + 2NO_2 + O_2$$

Thus, metallic silver clusters formed in alginate are believed to act as a kind of cross-linking agent, leading to the formation of new thermal transition temperature (Kwon *et al.*, 2005). However, one of the most important properties of wound dressing materials is the ability to maintain a sufficient content of water and due to a certain amount of free water contained in the samples, all spectra give a

significant transition at about 100°C except the silver nitrate. The identification of this transition peak implies that the good moisture-retention of the alginate is not affected by the addition of silver nitrate.

4.4.3 Morphology and Silver Content on the Fiber Surface

The surface morphologies of the fibers were observed using SEM micrographs. Figure 4.3 demonstrates SEM images of neat alginate fiber and silver-coated alginate fibers containing different amounts of silver nitrate. The average diameters of prepared fibers are ranged from 33 to 37 μm and did not change with the increase in the silver nitrate content. In contrast to the fiber diameters, Figure 4.3 also shows that an increase of the silver nitrate content has a dramatic effect on the dispersion of silver particles.

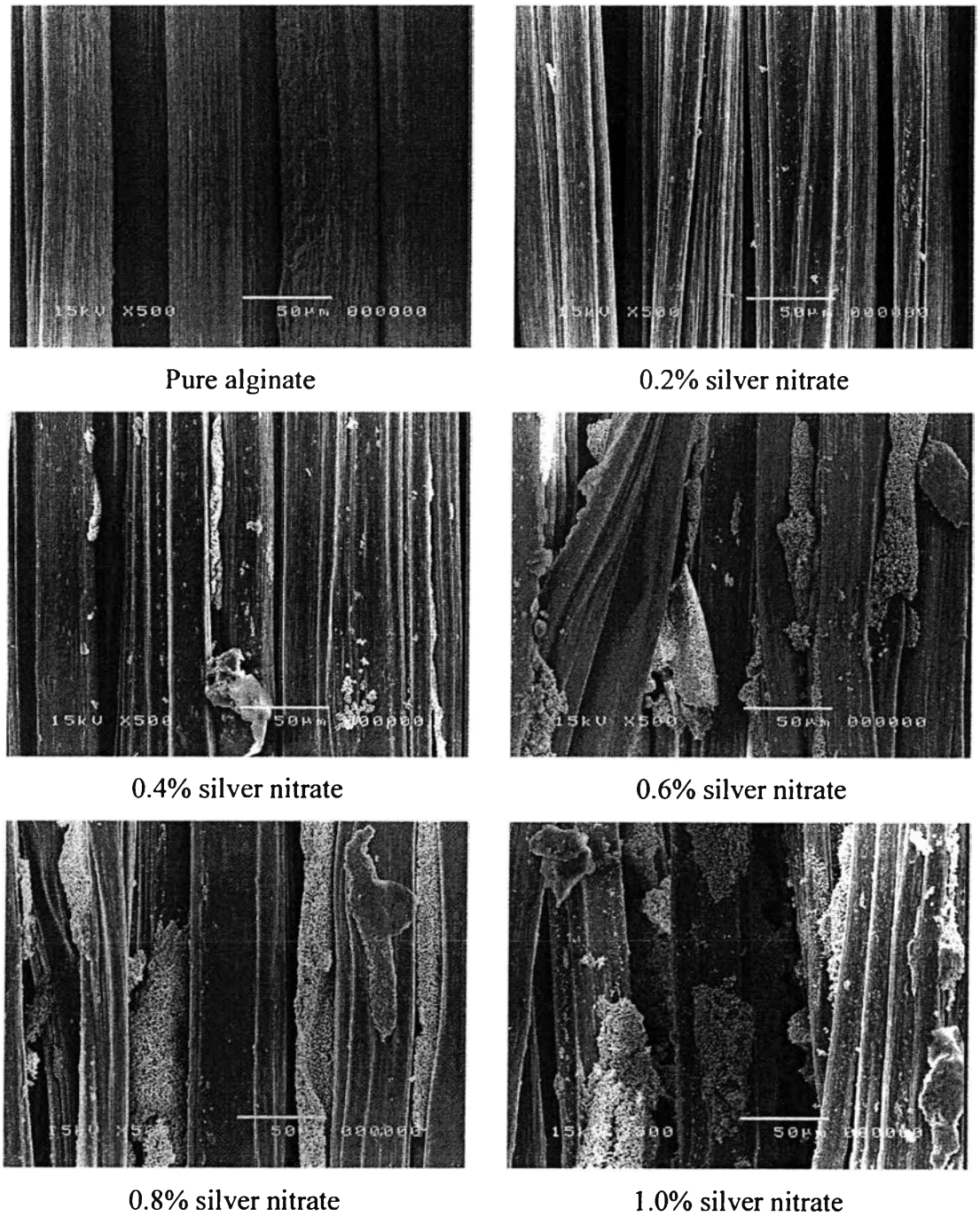

Figure 4.3 SEM images of neat alginate fiber and silver-coated alginate fibers containing different amounts of silver nitrate, at a magnification of 500x.

As expected, it was observed that an increase of the silver nitrate content in the 2nd coagulation bath had increased the amount of silver particles retained by the alginate fibers. However, it is also clear that evenly dispersion of

silver particles was observed only at the silver nitrate contents of 0.2% and 0.4% w/v. Interestingly, the size of silver particles in these two compositions are very small. They are silver nanoparticles consisting of both sphere and cylindrical rods which exhibited broad distribution in both of their length and width. The width of these silver nanoparticles ranged from 90 to 591 nm, while the length ranged from 106 to 799 nm. Statistical evaluation of the results suggested the average width and length of these silver nanoparticles to be about 230 and 316 nm, respectively (see Figure 4.4).

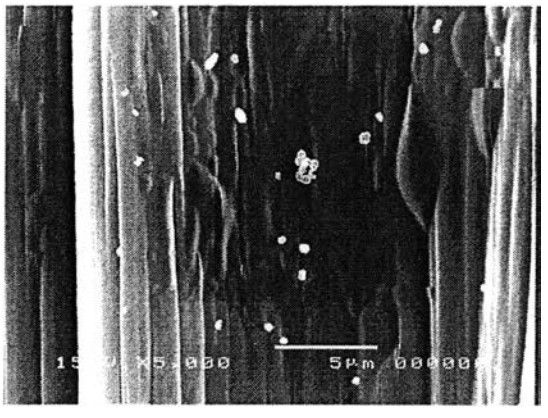

Figure 4.4 SEM image shows evenly dispersion of silver nanoparticles observed at the silver nitrate content of 0.2% w/v, at a magnification of 5000x.

When the silver nitrate content increased, the formation of larger silver agglomerates which are not uniformly dispersed within the alginate fiber surface occurred. This effect was confirmed from an energy-dispersive spectroscopy (EDS) analysis. The mapping of alginate fibers with the average value of 30 selected areas on silver and other elements showed in Figure 4.5 indicates the surface dispersion ratio on C, O, Cl, Ca, and Ag elements. As silver nitrate contents increase the amount of C element did not change remarkably while O and Ca element contents decreased gradually. This is due mainly to the significant increase in the ratio of the Ag element. In addition, when Ag element content increased the amount of Cl element also increased. The reason is due to double displacement reaction that occurred during the transportation of the fibers from the 1st coagulation bath to the

2nd coagulation bath. In this type of reaction, elements from two compounds displace each other to form new compounds. Double displacement reactions may occur when one product is removed from the solution as a gas or precipitate or when two species combine to form a weak electrolyte that remains undissociated in solution. Double displacement reaction occurs when solutions of calcium chloride and silver nitrate are reacted to form insoluble silver chloride in a solution of calcium nitrate was shown below (Helmenstein, 2006).

$$CaCl_2\,(aq) + 2\,AgNO_3\,(aq) \longrightarrow Ca(NO_3)_2\,(aq) + 2\,AgCl\,(s)$$

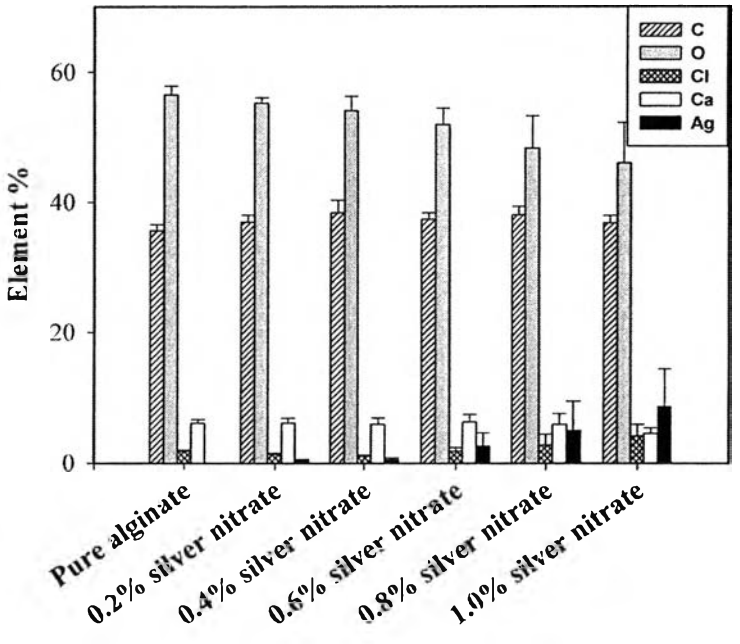

(A) The surface dispersion ratio of all elements.

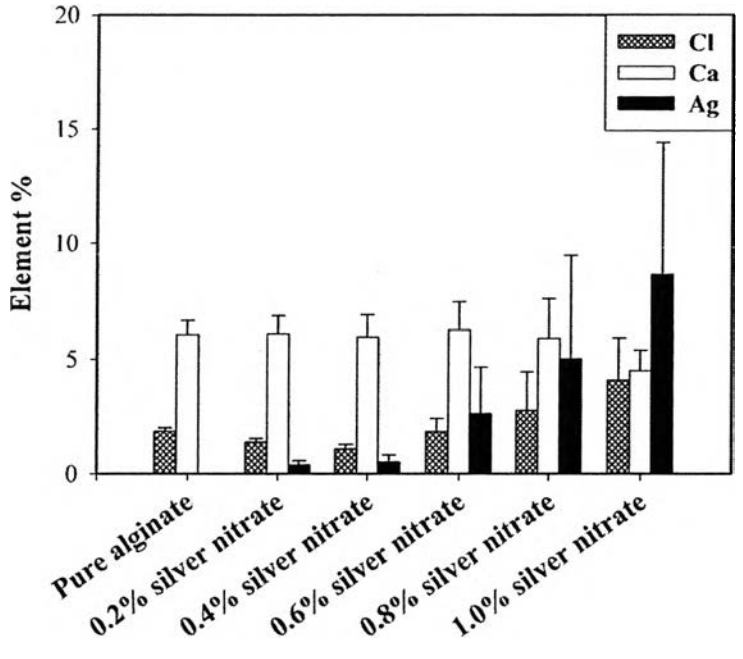

(B) The magnifying view of the surface dispersion ratio on Cl, Ca, and Ag elements.

Figure 4.5 EDS analysis indicates the surface dispersion ratios on C, O, Cl, Ca, and Ag elements of neat alginate fiber and silver-coated alginate fibers containing different amounts of silver nitrate.

Experiments by Gupta *et al.* (1998) have shown the effect of chloride on the availability of Ag^+ against *E. coli*. They showed that at low chloride levels, silver is excluded by precipitating as AgCl resulting in decreased Ag^+ resistance. In contrast, at high chloride concentrations, there is an increase in the proportion of water soluble complex anions, $AgCl_2^-$ and $AgCl_3^{2-}$ (Cotton and Wilkinson, 1988) that might have increased access to the cell membrane of microorganisms, resulting in increased bioavailability of Ag^+.

The uniformity of dispersion of silver particles was observed by considering standard deviation values of silver element contents for each coated fiber composition. The higher the standard deviation values, the less uniform dispersion of silver particles, was shown when $AgNO_3$ content increased.

4.4.4 Mechanical Integrity

In a continuous fiber composite, the tensile strength depends on the ability of the matrix to transfer stress to the filler through shearing at the filler/matrix interface, at a filler fracture. In this way the reinforcing efficiency of the filler is maintained (Johnson *et al.*, 2006). Figures 4.6 and 4.7 show the tenacity and the percentage of elongation at break of alginate yarn and silver-coated alginate yarns having silver nitrate content in the range of 0.2 - 1.0% w/v.

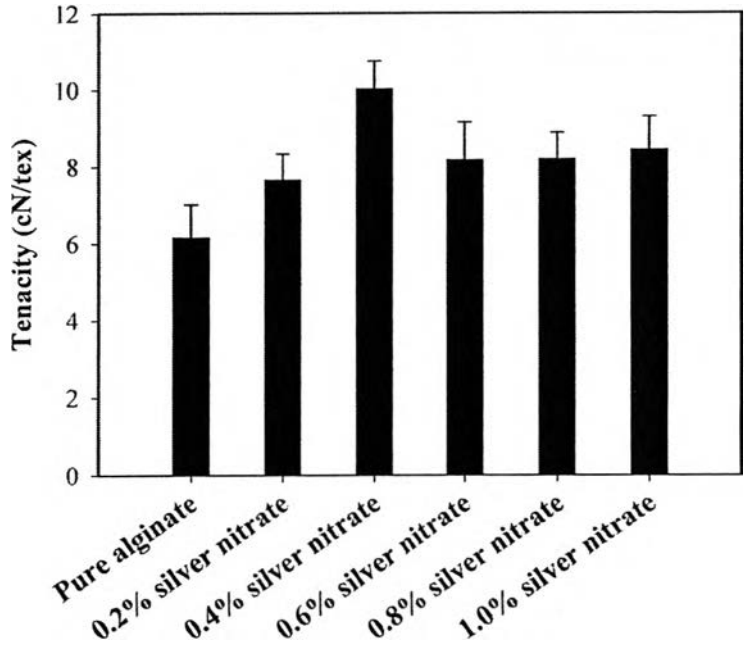

Figure 4.6 Tenacity of neat alginate yarn and silver-coated alginate yarns containing different amounts of silver nitrate.

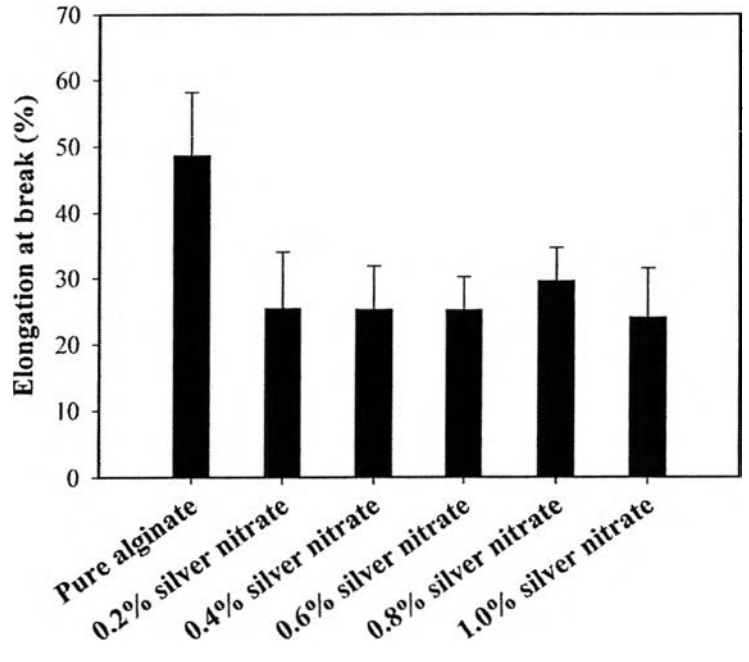

Figure 4.7 Percentage of elongation at break of neat alginate yarn and silver-coated alginate yarns containing different amounts of silver nitrate.

The tenacity of the coated yarns initially increased from that of the neat alginate yarn with an increase in the silver nitrate content to reach a maximum value at a silver nitrate content of 0.4% w/v and decreased gradually with further constant. Contrary to the tenacity, the percentage of elongation at break decreased from that of the pure alginate with an initial increase in the silver nitrate content and leveled off when the silver nitrate content was greater than or equal to 0.2% w/v.

The increase in the tenacity of the coated yarns at low silver content is due to the highly homogeneous distribution of silver particles. Besides, confirmed with SEM pictures, nanoparticle silver was observed at a small proportion of silver coated on alginate yarns (i.e. 0.2% w/v and 0.4% w/v) leading to the higher specific surface available for allowing the good stress transfer from the matrix to the fillers. As the surface area is increased, the filler-matrix adhesion is improved, resulting in a decrease in the mobility of the macromolecules. Therefore, the percentage of elongation at break tends to reduce gradually. On the other hand, if the filler matrix adhesion is very strong, fillers restrict the mobility of the matrix molecules (Premalal *et al.*, 2002). The decrease in the tenacity after that was because silver particles are mainly retained as agglomerates on the fiber surfaces, thus hindering the interactions in the fibers.

4.4.5 Antibacterial Activity

The antibacterial activities of silver-coated alginate fibers against gram-positive *S. aureus* and gram-negative *E. coli* were qualitatively investigated by observing the clear zones between the fibers and luxuriant bacteria colonies and the results are shown in Figures 4.8 and 4.9. Moreover, the width of clear zones was measured to consider the effect of silver content and Figure 4.10 shows the influence of silver content on the antibacterial capacities.

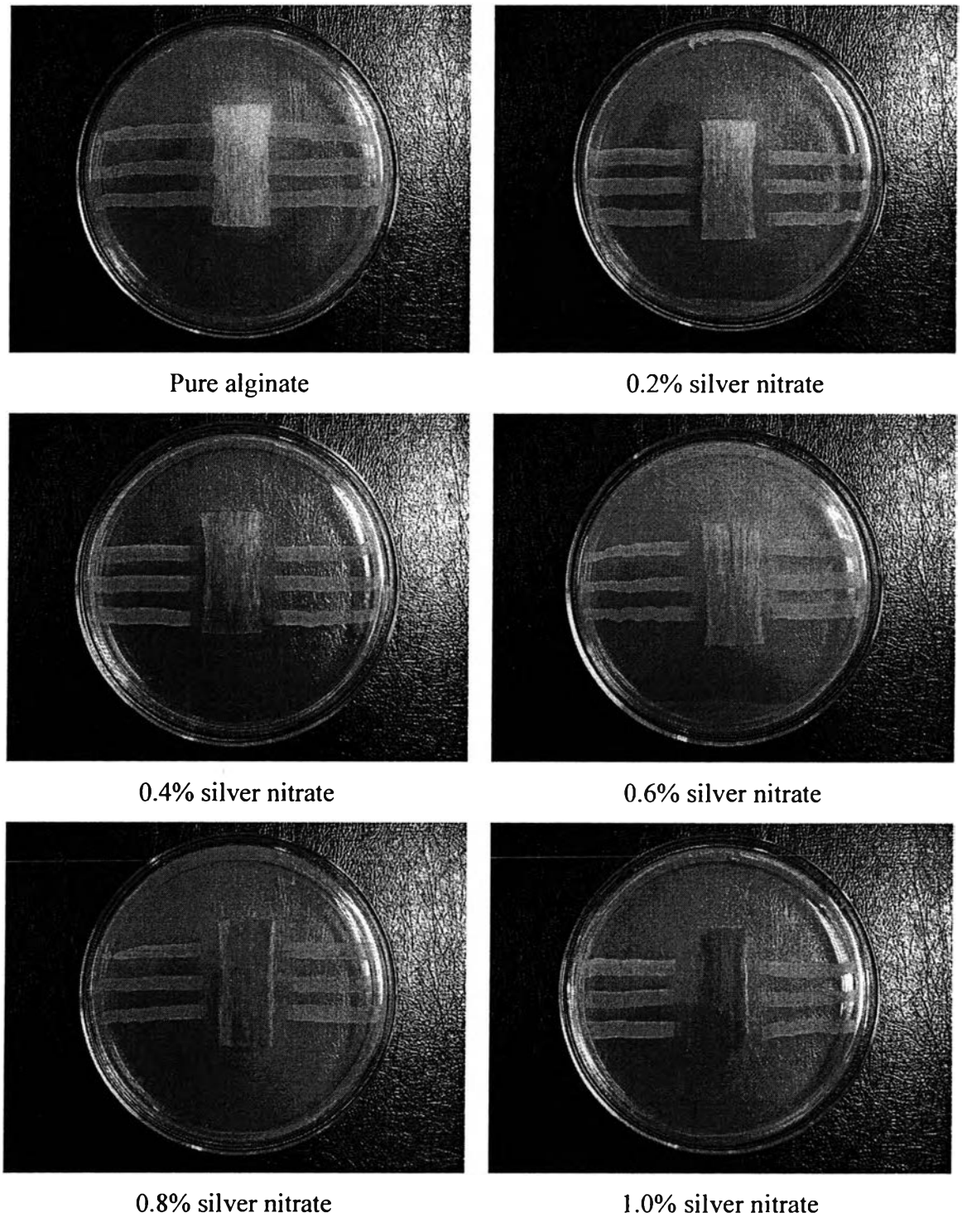

Figure 4.8 Antibacterial activities of neat alginate fiber and silver-coated alginate fibers containing different amounts of silver nitrate against *S.aureus*.

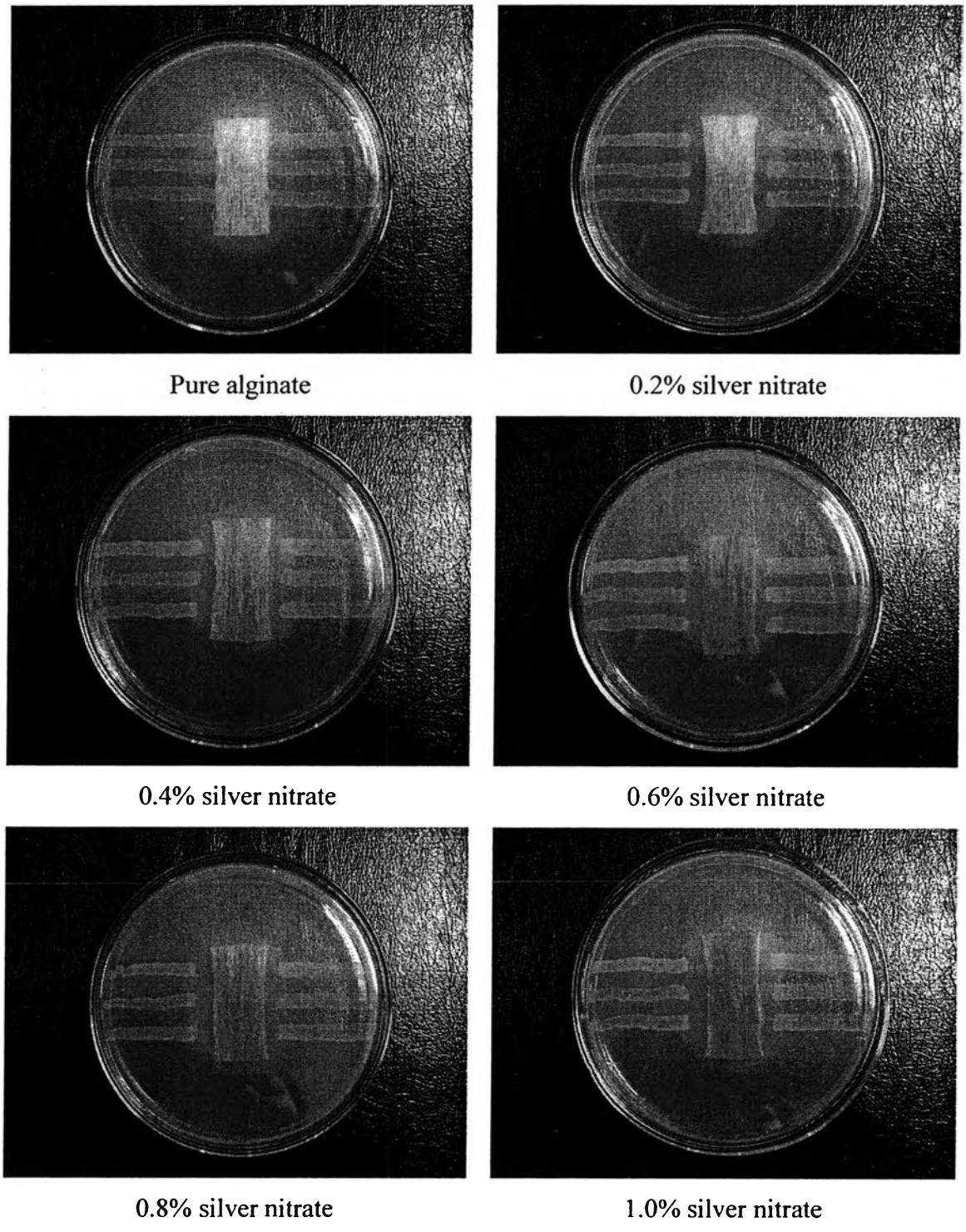

Figure 4.9 Antibacterial activities of neat alginate fiber and silver-coated alginate fibers containing different amounts of silver nitrate against *E. coli*.

According to Figures 4.8 and 4.9, neat alginate fibers exhibited no inhibitory zones while silver-coated alginate fibers showed inhibitory effect against both microorganisms. In addition, Figure 4.10 shows that all compositions of the coated fibers exhibit high efficiency of bacterial control and the antibacterial capacities increase with increasing the silver content, indicating that the silver particles are responsible for the antibacterial activity of the coated fibers and this activity is quite strong. Relatively, the antibacterial efficiency against *E. coli* is lower than that of against *S. aureus*, probably because of the difference in cell walls between gram-positive and gram-negative bacteria. The cell wall of *E. coli*, which consists of lipids, proteins and lipopolysaccharides (LPS), provides effective protection against biocides. However, the cell wall of gram-positive bacteria, such as *S. aureus*, does not consist of LPS (Speranza *et al.*, 2004).

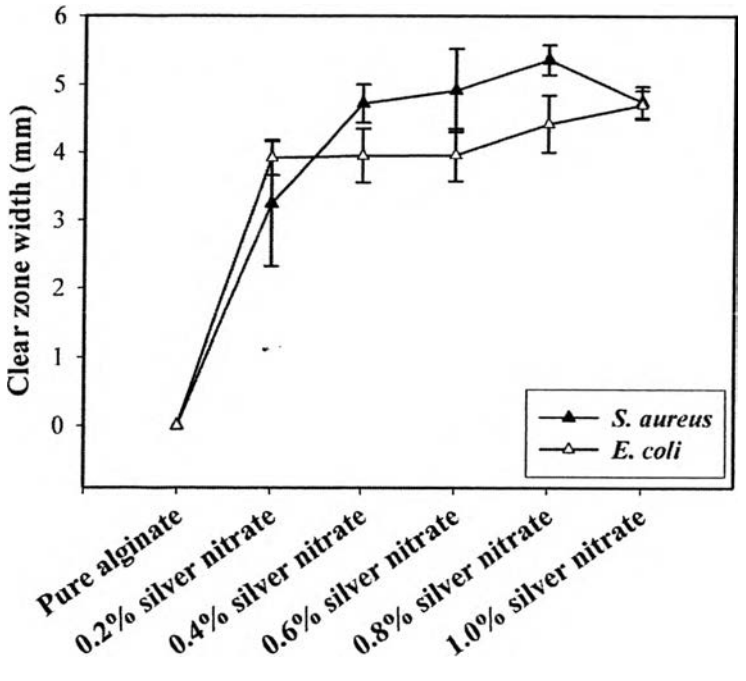

Figure 4.10 Influence of the silver content on antibacterial capacities of silver-coated alginate fibers containing different amounts of silver nitrate against *S. aureus* and *E. coli*.

4.5 Conclusions

Antibacterial silver-coated alginate fibers can be obtained by spinning viscose alginate solution through the solution of silver nitrate using the wet spinning process. The interactions between silver nitrate and alginate molecules are electrostatic interactions, namely ion-dipole interactions, occur between acetate groups of alginate and electropositive silver metal cations. The study of the properties of the silver-coated alginate fibers has revealed that using small proportions of silver nitrate exhibited a much higher tenacity than those using the higher silver nitrate contents, because of the highly homogeneous distribution of silver particles and the higher specific surface available for allowing the good stress transfer from the matrix to the fillers. Besides, the good moisture-retention of the alginate is not affected by the addition of silver nitrate and all compositions of the coated fibers show high efficiency of bacterial control against both gram-positive *S. aureus*, and gram-negative *E. coli*. All of these reasons indicate that the present-prepared silver-coated alginate fibers show high potential application as wound dressings.

4.6 Acknowledgements

Financial support from the Petroleum and Petrochemical College, Chulalongkorn University and the Development and Promotion of Science and Technology Talent Project (DPST) is gratefully acknowledged.

4.7 References

Anonymous, "Alginic acid". 2007 <http://en.wikipedia.org/wiki/Alginic_acid>

Bragg, P.D., and Rainnie, D.J. (1974) The effect of silver ions on the respiratory chain of *E. coli*. Canadian Journal of Microbiology, 20(6), 883-889.

Clare, K. (1993) In R.L. Whistler, and J.N. BeMiller (Eds.), Industrial gums: Polysaccharides and their derivatives, San Diego: Academic Press, 105-143.

Clement, J.L., and Jarrett, P.S. (1994) Antibacterial silver. Metal-Based Drugs, 1, 467-482.

Cotton, F.A., and Wilkinson, G. (1988) Advanced Inorganic Chemistry. In John Wiley and Sons: Silver and gold: group IB(11), 5th Ed. (937-949). Inc: New York, N.Y.

Darouiche, R.O. (1999) Anti-infective efficacy of silver-coated medical prostheses. Clinical Infectious Diseases, 29(6), 1371-1377.

Dunn, K., and Jones, V.E. (2004) The role of Acticoat™ with nanocrystalline silver in the management of burns. Burns, 30(suppl. 1), S1-59.

Galeano, B., Korff, E., and Nicholson, W.L. (2003) Inactivation of vegetative cells, but not spores, of *Bacillus anthracis*, *B. cereus*, and *B. subtilis* on stainless steel surfaces coated with an antimicrobial silver- and zinc-containing zeolite formulation. Applied and Environmental Microbiology, 69, 4329-4331.

Gaonkar, T.A., Sampath, L.A., and Modak, S.M. (2003) Evaluation of the antimicrobial efficacy of urinary catheters impregnated with antiseptics in an in vitro urinary tract model. Infection Control and Hospital Epidemiology, 24, 506-513.

George, N., Faoagali, J., and Muller, M. (1997) Silvazine™ (silver sulfadiazine and chlorhexidine) activity against 200 clinical isolates. Burns, 23(6), 493-495.

Guggenbichler, J.P., Boswald, M., Lugauer, S., and Krall, T. (1999) A new technology of microdispersed silver in polyurethane induces antimicrobial activity in central venous catheters. Infection, 27(Suppl. 1), S16-23.

Gupta, A., Maynes, M., and Silver, S. (1998) Effects of halides on plasmid-mediated silver resistance in *Escherichia coli*. Applied and Environmental Microbiology, 64(12), 5042-5045.

Gupta, A., and Silver, S. (1998) Silver as a biocide: will resistance become a problem? Nature Biotechnology, 16, 888.

Helmenstein, A.M. "Reactions in water or aqueous solution." About.com: chemistry Aug 2006 <http://chemistry.about.com/cs/generalchemistry/a/aa072103a>

Holt, K.B., and Bard, A.J. (2005) Interaction of silver(I) ions with the respiratory chain of *Escherichia coli*: an electrochemical and scanning electrochemical microscopy study of the antimicrobial mechanism of micromolar Ag^+. Biochemistry, 44(39), 13214-13223.

Horncastle, J. (1995) Wound dressings: Past, present, and future. Medical Device Technology, Jan/Feb, 30-36.

Jarvis, P.M., Galvin, D.A.J., Blair, S.D., and McCollum, C.N. (1987) How does calcium alginate achieve hemostasis in surgery? Thrombosis and haemostasis, 58(1), 80.

Johnson, A.C., Zhao, F.M., Hayes, S.A., and Jones, F.R. (2006) Influence of a matrix crack on stress transfer to an α-alumina fiber in epoxy resin using FEA and photoelasticity. Composites Science and Technology, 66, 2023-2029.

Kodokawa, J.I., Saitou, S., and Shoda, S.I. (2005) Preparation of alginate-polymethacrylate hybrid material by radical polymerization of cationic methacrylate monomer in the present of sodium alginate. Carbohydrate Polymers, 60, 253-258.

Kwon, J.W., Yoon, S.H., Lee, S.S., Seo, K.W., and Shim, I.W. (2005) Preparation of silver nanoparticles in cellulose acetate polymer and the reaction chemistry of silver complexes in the polymer. Bulletin of the Korean Chemical Society, 26(5), 837-840.

Lever, A.B.P., Mantovani, E., and Ramas, W.B.S. (1971) Canadian Journal of Chemistry-Revue Canadienne De Chimie, 49.

Lloyd, L.L., Kennedy, J.F., Methacanon, P., Paterson, M., and Knill, C.J. (1998) Carbohydrate polymers as wound management aids. Carbohydrate Polymers, 37, 315-322.

McDowell, R.H. (1974) In Properties of Alginates, 3rd Ed. Alginate Industry Limited: London.

Miraftab, M., Qiao, Q., Kennedy, J.F., Anand, S.C., and Groocock, M.R. (2003) Fibres for wound dressings based on mixed carbohydrate polymer fibres. Carbohydrate Polymers, 53, 225-231.

Miura, K., Kimura, N., Suzuki, H., Miyashita, Y., and Nishio, Y. (1999) Thermal and viscoelastic properties of alginate/poly(vinyl alcohol) blends cross-linked with calcium tetraborate. Carbohydrate Polymers, 39, 139-144.

Percival, S.L., Bowler, P.G., and Russell, D. (2005) Bacterial resistance to silver in wound care. Journal of Hospital Infection, 60, 1-7.

Premalal H.G.B., Ismail, H., and Baharin, A. (2002) Comparison of the mechanical properties of rice husk powder filled polypropylene composites with talc filled polypropylene composites. Polymer Testing, 21, 833-839.

Qin, Y., and Gilding, D.K. (1996) Alginate fibres and wound dressings. Medical Device Technology, Nov, 32-40.

Ribeiro, A.J., Silva, C., Ferreira, D., and Veiga, F. (2005) Chitosan-reinforced alginate microspheres obtained through the emulsification/internal gelation technique. Pharmaceutical Sciences, 25, 31-40.

Shimizu, T., and Takada, A. (1997) Preparation of Bi-based superconducting fiber by metal biosorption of Na-alginate. Polymer Gels and Networks, 5, 267-283.

Smitha, B., Sridhar, S., and Khan, A.A. (2005) Chitosan-sodium alginate polyion complexes as fuel cell membranes. European Polymer Journal, 41, 1859-1866.

Speranza, G., Gottardi, G., Pederzolli, C., Lunelli, L., Canteri, R., Pasquardini, L., Carli, E., Lui, A., Maniglio, D., Brugnara, M., and Anderle, M. (2004) Role of chemical interactions in bacterial adhesion to polymer surfaces. Biomaterials, 25, 2029-2037.

Thomas, S., and McCubbin, P. (2003) A comparison of the antimicrobial effects of four silver-containing dressings on three organisms. Journal of Wound Care, 12, 101-107.

Winter, G.D. (1962) Formation of the scab and the rate of epithelialization of superficial wounds in the skin of the young domestic pig. Nature, 193, 293-294.

Zamali, H., Rogez, J., Bergman, C., and Mathieu, J.C. (1998) Heat capacities and enthalpies of transition of $AgNO_3$. Thermochimica Acta, 311, 37-41.

Zohuriaan, M.J., and Shokrolahi, F. (2004) Thermal studies on natural and modified gums. Polymer Testing, 23, 575-579.